Statut report on cluster finding and Kalman Filter based track reconstruction in the forward Muon spectrometer of ALICE

by
K. Boudjemline , G. Chabratova , J-P Cussonneau
C. Finck , M Germain , V. Kekelidze , L. Luquin
P. Lautridou , D. Thers , A. Vodopianov , A. Zinchenko
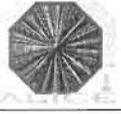
Status report

on cluster finding and Kalman filter based

track reconstruction

in the forward muon spectrometer of ALICE

K. Boudjemline[2], G. Chabratova[1], J.P. Cussonneau[2], Ch. Finck[2],
M. Germain[2], V. Kekelidze[1], P. Lautridou[2], L. Luquin[2], D. Thers[2],
A. Vodopianov[1], A. Zinchenko[1]

[1]*JINR, Dubna, Russia*

[2]*SUBATECH, Nantes, France*

Abstract

An algorithm of hit finding in muon chambers of the forward muon spectrometer is described. Some preliminary results on its performance are shown. Current status of the track reconstruction based on Kalman filtering approach is presented.

1 Hit finding algorithm

1.1 Maximum Likelihood - Expectation Maximization algorithm

The hit finding algorithm is based on a Maximum Likelihood - Expectation Maximization (MLEM) technique[1] (also known as Bayesian unfolding[2]). It effectively allows to improve the detector segmentation (i.e. decrease cathode pad size), offering better conditions for making a decision about complex cluster splitting.

The algorithm starts from finding groups of adjacent pads on one cathode and overlapping with them pads on the other cathode which together form a "precluster" (Fig. 1). For a given precluster an array of pixels in the anode plane is built with the size defined by the overlap of pads on both cathodes. It is assumed that each pixel contains a track. If the initial value of energy release from a track j (i.e. pixel intensity) was p_j^0 (usually all p_j^0's are set to 1) then the following iterative procedure will update its value:

$$p_j^{k+1} = \frac{p_j^k}{\sum\limits_{i=1}^{N_{pads}} c_{ij}} \sum_{i=1}^{N_{pads}} c_{ij} \frac{q_i}{f_i^k} \quad \text{with} \quad f_i^k = \sum_{j=1}^{N_{pix}} c_{ij} p_j^k, \tag{1}$$

where f_i^k is the expected signal on pad i if the pixel intensity was p_j^k (at the kth iteration), c_{ij} is the pixel-to-pad coupling (given by Mathieson integral) and N_{pix} is the number of pixels in the array.

After several iterations (10-15) the larger pixel dimension is decreased by two and pixels with the lowest intensity are removed if the total number of pixels exceeds the number of pads. This is necessary in order to ensure the unique solution of the system. Then the iterative procedure is performed again. The algorithm stops when the pixel size becomes sufficiently small (1 mm) (see Fig. 2).

1.2 Cluster splitting

The found groups of pixels are taken as the seeds for the standard Mathieson fit. Currently, up to 3-point Mathieson fit is used to ensure the good convergence of the MINUIT procedure. If number of seeds is more than 3, the splitting of the precluster is needed which can be done as follows. Let us define cluster$_i$-to-pad$_j$ coupling

$$c_{ij}^{c-p} = \sum_{k=1}^{N_{pix}^i} c_{kj}, \tag{2}$$

where c_{kj} is the pixel-to-pad coupling as in Eq.(1), and cluster$_i$-to-cluster$_j$ coupling

$$c_{ij}^{c-c} = \sqrt{\sum_{k=1}^{N_{pads}} c_{ik}^{c-p} c_{jk}^{c-p}} \tag{3}$$

1

Then the group of 1, 2 or 3 clusters is selected with the minimum total coupling to all the others. For the selected clusters the pads coupled to them and weakly coupled to the others are taken to perform the Mathieson fit. If there were pads with strong coupling to the selected group and all the others their charge is corrected for the contribution from the fitted clusters. The remaining clusters are split again if necessary.

1.3 Fitting procedure

If N seeds are selected by the procedure described above (N=1-3), the N- and N-1-point Mathieson fits are performed. If N=3 and χ^2/N_{dof} of the N-1-point fit is lower the N-2-point fit is done as well. Results form the fit with the lowest χ^2/N_{dof} are taken as the final ones. The number of free parameters is chosen to be $3N$-1 since there is a constrain of conservation of the total cluster charge.

The exact expression minimized by MINUIT is the following:

$$"\chi^{2"} = \sum_i^{N_{pads}} \frac{(q_i - f)^2}{q_i \, \bar{q}} \tag{4}$$

where q_i is the pad charge, f is its estimation by the fitted function and $\bar{q} = \frac{1}{N_{pads}} \sum_i^{N_{pads}} q_i$ is the average cluster charge. As has been found it gives better results that the one currently used:

$$"\chi^{2"} = \sum_i^{N_{pads}} \left(\frac{q_i - f}{q_i} \right)^2 \tag{5}$$

1.4 Results

The results obtained are shown in Figs. 3, 4, where the hit residuals (differences of the reconstructed and simulated hit coordinates) are shown. One can see, that the proposed method gives noticeable improvement especially for high background contamination. It should be noted that the narrower peak in bending plane results from the new fitted function whereas the new cluster finding algorithm reduces the distribution tails.

2 Kalman filter

2.1 Basic formalism

Description of the Kalman filter as a track reconstruction method can be found, for instance, in [3]. The tracking procedure is briefly outlined below.

The algorithm starts from track candidates ("seeds"), for which vectors of initial parameters p and weight matrices $\mathbf{W} = \mathbf{C}^{-1}$ are estimated with $\mathbf{C}$ being the covariance matrix estimate. Then each track is propagated to some surface (detector or intermediate

point). If p^e is a vector of propagated parameters the new weight matrix $\mathbf{W}^e$ can be obtained as

$$\mathbf{W}^e = (\mathbf{D}^{-1})^t \mathbf{W} \mathbf{D}^{-1}, \tag{6}$$

where $\mathbf{D}$ is the Jacobian matrix of the transformation, i.e. the matrix of derivatives of propagated track parameters with respect to current parameters, given by

$$\mathbf{D} = \partial p^e / \partial p. \tag{7}$$

A new measurement with the vector of local measured parameters m and its weight matrix $\mathbf{U}$ can be added according to the equation:

$$(\mathbf{W} + \mathbf{U})(p' - p) = \mathbf{U}(m - p), \tag{8}$$

where p' is the vector of track parameters after adding the new measurement. The new weight matrix and χ^2-value are:

$$\mathbf{W}' = \mathbf{W} + \mathbf{U} \tag{9}$$

and

$$\chi'^2 = \chi^2 + (p' - p)^t \mathbf{W}(p' - p) + (p' - m)^t \mathbf{U}(p' - m), \tag{10}$$

respectively.

2.2 Kalman filter implementation for the forward muon spectrometer within the AliROOT framework

A Kalman track seed (class *AliMUONTrackK*) is created for all track segments found in detector stations 4 and 5[4]. Tracks are parameterized as $(y, x, \alpha, \beta, q/p)$, where y is a coordinate in the bending plane, x is a non-bending coordinate, α is a track angle in the bending plane with respect to the beam line, β is an angle between the track and the bending plane, q and p are the track charge and momentum, respectively. Then the seed's covariance matrix can be estimated as

$$\mathbf{C} = \begin{pmatrix} \sigma_y^2 & 0 & \dfrac{\sigma_y^2}{(1 + \tan^2 \alpha)\Delta z} & 0 & 0 \\ & \sigma_x^2 & 0 & \dfrac{\sigma_x^2 \cos \alpha}{(1 + \tan^2 \beta)\Delta z} & 0 \\ & & \dfrac{2\sigma_y^2}{((1 + \tan^2 \alpha)\Delta z)^2} & 0 & 0 \\ & & & \dfrac{2\sigma_x^2 \cos^2 \alpha}{((1 + \tan^2 \beta)\Delta z)^2} & 0 \\ & & & & (0.5q/p)^2 \end{pmatrix}, \tag{11}$$

where σ_y and σ_x are the measurement errors in bending and non-bending planes, respectively, Δz is the z-coordinate difference of the hits on the segment and the error of q/p

was taken to be "sufficiently large" (50% of the value itself).

A track starting in station 5 is followed to the station 1 or until it is lost (if no hits in a station are found for this track). If the track starts in station 4 it is followed to the station 5, propagated back to the station 4 (in current implementation the track picks up the old hits in station 4 - no search for better hits is performed) and followed as usually.

In order to take into account the realistic track chamber segmentation the propagation procedure is written as follows. It propagates the track from the current z-position to a hit with the nearest z-coordinate. Then for given z it looks for the hits within certain window around the transverse track position (the window is taken to be 4σ) and calculates the χ^2-contribution of each hit. The hit giving the lowest contribution is taken as belonging to the track.

Since the magnetic field is non-uniform, the Runge-Kutta algorithm is used for propagation of track parameters. It is also used to calculate the Jacobian matrix according to the formula:

$$D^{10} \equiv \partial P^1 / \partial P^0 = \Delta P^1 / \Delta P^0, \tag{12}$$

where D^{10} is a Jacobian matrix element and ΔP^1 is a change of the propagated parameter P^1 for the given change ΔP^0 of the current parameter P^0.

Effect of the track chamber material is taken into account by adding a multiple scattering term to the track covariance matrix for each chamber traversed. In the thin layer approximation this term can be written as

$$\mathbf{C}^{MS} = diag\ (0,\ 0,\ \theta_{MS}^2 / \cos^2 \beta,\ \theta_{MS}^2,\ 0), \tag{13}$$

where θ_{MS} is the projected scattering angle.

After propagation to the chamber 1 all tracks are sorted according to their quality, defined as

$$Quality = N_{hits} + \frac{\chi_{max}^2 - \chi^2}{\chi_{max}^2 + 1}, \tag{14}$$

where χ_{max}^2 is the maximum acceptable χ^2 of tracks. Then duplicated tracks are removed, where duplicated means having half or more of their hits shared with the other tracks.

The remaining tracks are propagated through the absorber to the vertex using either the *AliMUONTrackParam::BransonCorrection* method or the Kalman propagator (the latter currently using material constants taken from the former one) with the vertex being used as an additional point. The contribution of the multiple scattering in the absorber to the covariance matrix is calculated according to the formula[5]:

$$C_{kl}^{MS} = \theta_0^2 \int_L \ (\frac{\partial p_k}{\partial \beta} \frac{\partial p_l}{\partial \beta} + \frac{\partial p_k}{\partial \theta} \frac{\partial p_l}{\partial \theta}) dl, \tag{15}$$

where p_k, p_l are track parameters, θ is the scattering angle orthogonal to β, θ_0 is the projected scattering angle per unit length and the integral is taken over the path length L in the material. Under assumption that effect of the magnetic field in the absorber is small, the tracks can be approximated as straight lines; in this case the integration in (15) can be done analytically. The resulting covariance matrix term due to multiple scattering

in the absorber is

$$\mathbf{C}^{MS} = \theta_0^2 \times \begin{pmatrix} \dfrac{L^3}{3}y_\theta{}^2 & \dfrac{L^3}{3}y_\theta x_\theta & \dfrac{L^2}{2}y_\theta\alpha_\theta & 0 & 0 \\[2ex] & \dfrac{L^3}{3}(x_\theta{}^2 + x_\beta{}^2) & \dfrac{L^2}{2}x_\theta\alpha_\theta & \dfrac{L^2}{2}x_\beta & 0 \\[2ex] & & L\alpha_\theta{}^2 & 0 & 0 \\[2ex] & & & L & 0 \\[2ex] & & & & 0 \end{pmatrix}, \tag{16}$$

with

$$y_\theta = \frac{1}{\cos\alpha}, \qquad x_\theta = \tan\alpha\tan\beta,$$
$$x_\beta = \frac{1}{\cos\beta}, \qquad \alpha_\theta = \frac{1}{\cos\beta}. \tag{17}$$

To account for track energy losses and material composition of the absorber the correction procedure is done for several material layers.

3   Some results

The results presented below were obtained for dimuons from upsilon decays for default detector parameters (*V3.06*: bending resolution 100 μm, non-bending resolution 1.44 mm, chamber efficiency 95%) and geometry as of *AliMUONv1*.

At first, only GEANT smeared hits were used leaving aside problems associated with the cluster finding and hit reconstruction. The single track efficiency for the case without background was found to be 97.8%, close to what is expected from the majority cut used in the track-finding algorithm (3 out of 4 chambers in the last two stations, 1 of 2 inside the magnet and 1 of 2 in the stations before the magnet) which gives 97.9% efficiency limit.

To get a feeling of how the track reconstruction behaves in a crowded environment, different number of background events were added to the signal. The results can be seen in Fig. 5, where the tracking efficiency for the muons from upsilon decays is shown along with the percentage of "bad" tracks, where "bad" means a signal track having at least one wrong hit association. The efficiency there is defined as percentage of reconstructed "reconstructable" tracks (i.e. tracks satisfying the hit majority cut). As can be seen this simplified test yields quite small number of bad tracks most of them with only one wrong hit. As a result, the mass resolution remains practically unaffected.

Performance of the Kalman filter in comparison with the default tracking program can be seen in Table 1. It is clear that the Kalman filter demonstrates similar tracking quality with much higher processing speed.

First tests with the "realistic" cluster finding and hit reconstruction algorithms demonstrated that the track finding efficiency of the Kalman filter for crowded events dropped down significantly as compared with the default tracking (Table 2). However, the track momentum and mass resolution were found to be much better (see Figs. 6, 7).

3.1 Algorithm modifications

The close examination of the lost tracks showed that their loss was due to wrong points which caused track distortion. There are several possible ways to improve the efficiency:

1. pick up all points inside the propagated window rather than the one with the lowest χ^2 contribution (make use of track "branching");

2. exclude the last found point on the track and try to find track continuation in the next chamber;

3. use better hit finding algorithm and/or better estimation of measurement errors in order to obtain correct weight of the points;

4. increase the acceptance window size and try to improve found tracks (remove "bad" hits) during backpropagation procedure

Implementation of modifications 1 and 2 has helped to increase the efficiency as can be seen in Table 2 (bottom row). Partial realization of modification 3 (as described in Sect. 1) has improved significantly both tracking methods (see Table 3 and Fig. 8). Effect of the 4th modification will be studied in near future.

4 Conclusions

The Kalman filter based method of track reconstruction has been developed for the AL-ICE forward muon spectrometer and implemented within the AliROOT framework.

Its tests for simulated events at the cluster level showed that its efficiency goes down for high multiplicity events leaving rather good mass resolution. Such a behaviour has been understood and several steps to recover the lost tracks have been implemented.

In order to further improve the tracking performance the cluster finding algorithm should (and can) be improved as well. Presented results of the proposed approach look quite promising and justify further work in this direction.

5 Acknowledgements

References

[1] L. A. Shepp and Y. Vardi, IEEE Trans. Med. Im., v.1, 1982, pp.113-122.

[2] G. D'Agostini, NIM A362 (1995) pp.487-498.

[3] P. Billoir and Q. Qian, Nucl. Instr. and Meth., A294 (1990) 219.

[4] ALICE Collaboration, CERN/LHCC/96-32 (1996).

[5] R.K. Bock et al., Data analysis techniques for high-energy physics experiments, University Press, Cambridge, 1990.

Default tracking, 1000 Upsilons			
Background level	0	1	2
Efficiency, %	97.8	97.9	97.1
Mass resolution, MeV	87.6±3.7	90.1±3.8	87.1±3.3
CPU time/event, sec	1.2	13.9	30.0
Kalman filter, 1000 Upsilons			
Background level	0	1	2
Efficiency, %	99.4	99.0	98.7
Mass resolution, MeV	83.2±3.2	86.9±3.4	83.2±3.2
CPU time/event, sec	0.3	2.2	6.7

Table 1: Performance results of the default tracking method and Kalman filter for GEANT smeared hits. Background level is expressed in terms of the nominal background events. Single track efficiency is shown defined with respect to the "reconstructable" tracks (see the text). Mass resolution is taken from the fit to the Gaussian in the range 9.3-9.8 GeV.

Default tracking, 2500 Upsilons			
Background level	0	1	2
Efficiency, %	94.0	91.4	83.7
Mass resolution, MeV	70.7±1.5	93.0±2.6	151.7±7.3
CPU time/event, sec	1.4	1.4	1.5
Kalman filter, 2500 Upsilons			
Background level	0	1	2
Efficiency, %	89.3	71.2	47.9
Mass resolution, MeV	69.5±1.5	77.6±2.2	96.3±5.6
CPU time/event, sec	0.6	0.6	0.5

Kalman filter, 7500 Upsilons			
Efficiency, %	-	82.1	63.1

Table 2: The same as Table 1 for the cluster level. Single track efficiency is shown defined with respect to the tracks generated within the detector acceptance. Bottom row shows results for the modified Kalman filter.

Default tracking, 1000 Upsilons			
Background level	0	1	2
Efficiency, %	94.5	92.9	90.7
Mass resolution, MeV	96.2±3.1	103.0±3.9	107.4±4.1
CPU time/event, sec	0.6	0.6	0.7
Kalman filter, 1000 Upsilons			
Background level	0	1	2
Efficiency, %	91.5	88.8	85.4
Mass resolution, MeV	93.6±3.5	92.8±3.6	95.8±3.8
CPU time/event, sec	0.2	0.2	0.2

Table 3: The same as Table 2 for hits reconstructed with the new cluster finder.
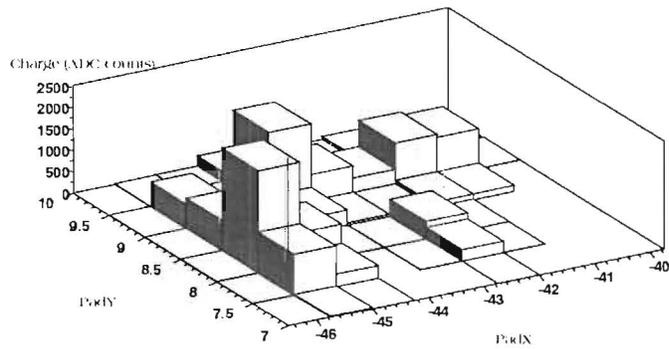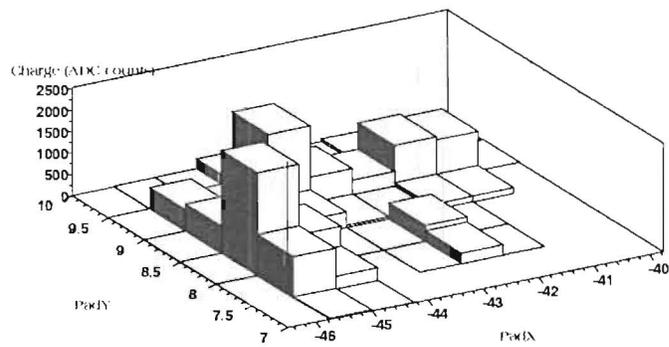
Figure 1: Example of a "precluster". Reconstructed hit positions are shown as the lines. The nearest line overlaps with the simulated hit position.
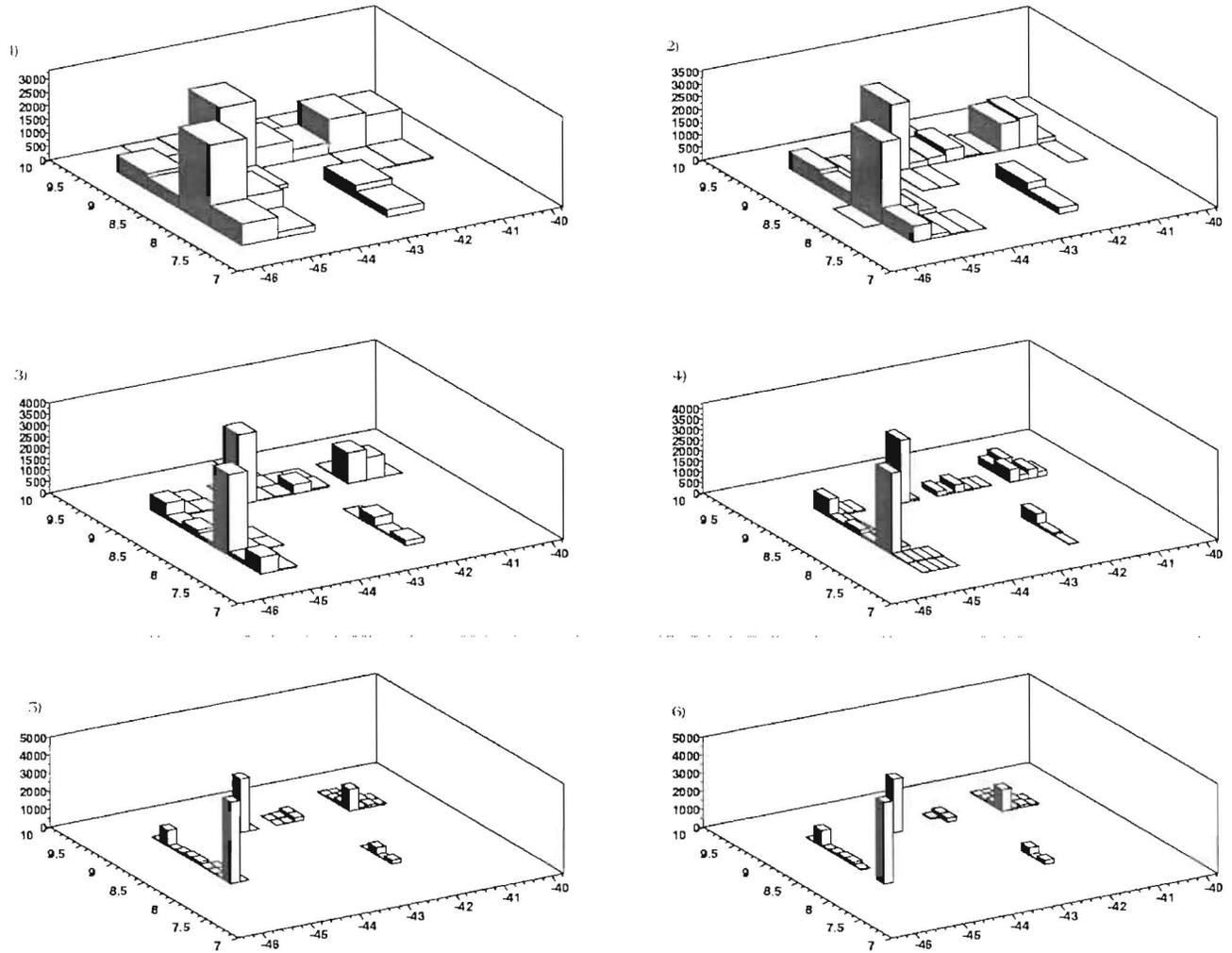
Figure 2: Pixel arrays found by the MLEM method on each pass for the precluster from Fig. 1.
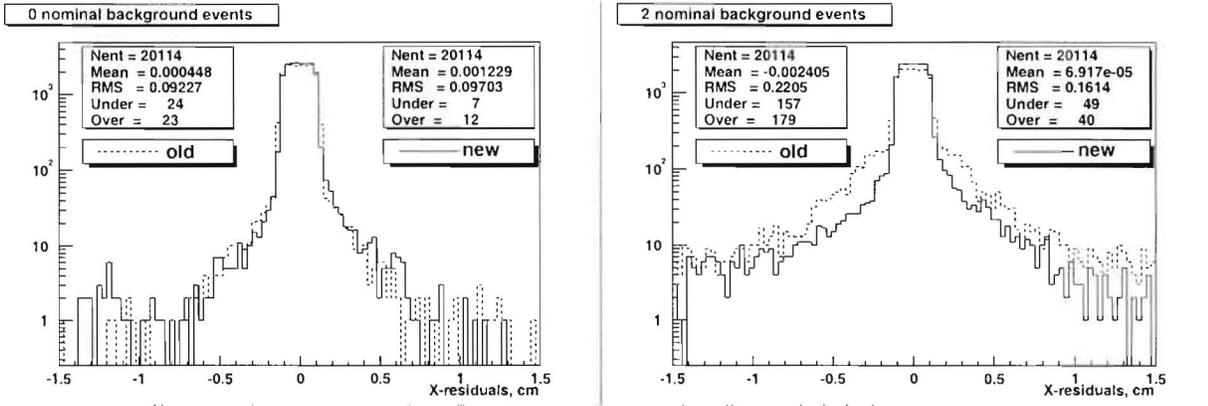
Figure 3: Residual distributions for non-bending plane. Solid histogram shows results for the new cluster finder, dashed for the old one. Left) only muons from upsilon decays are simulated, right) 2 nominal background events are added.
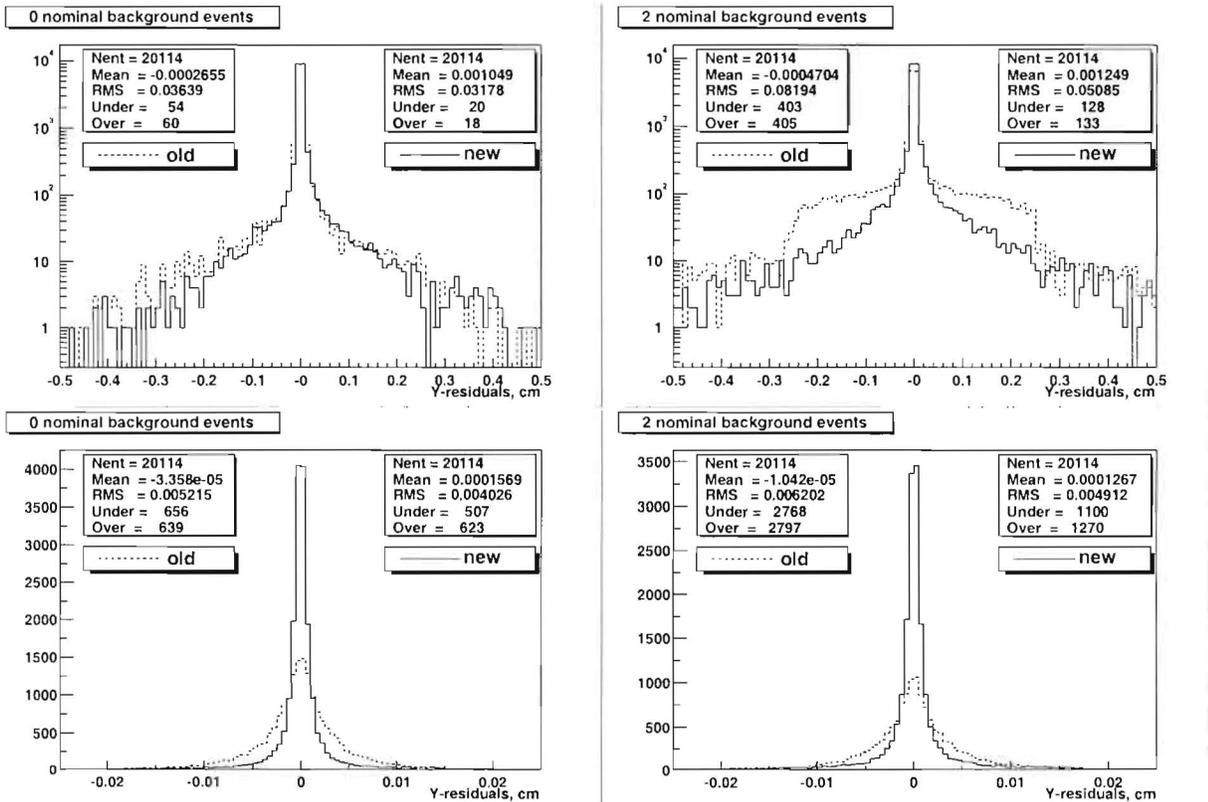
Figure 4: The same as in Fig. 3 for bending plane. Top and bottom rows are in log and linear scales.

11
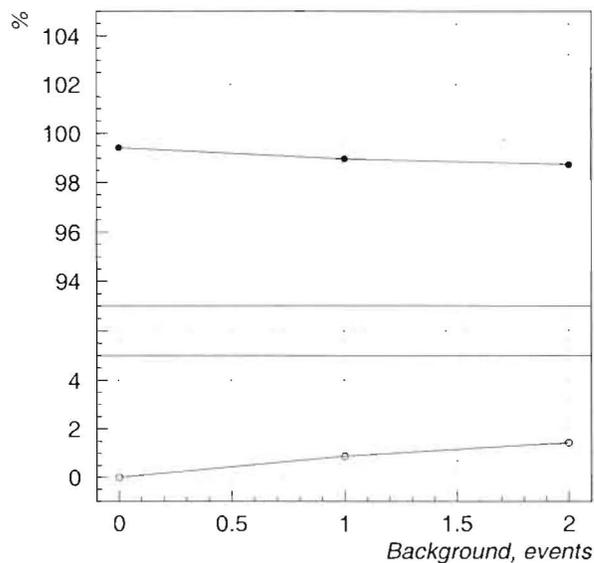
Figure 5: Tracking efficiency (closed circles) and percentage of "bad" tracks (open circles) versus occupancy, expressed in terms of the number of added background events.
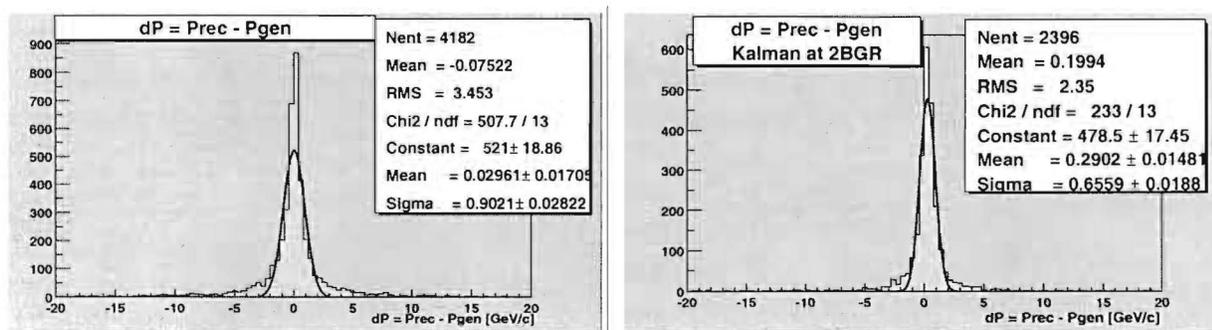
Figure 6: Distribution of difference of the reconstructed and generated track momenta for the case of "realistic" cluster finding and two background events: left) default tracking, right) Kalman filter.
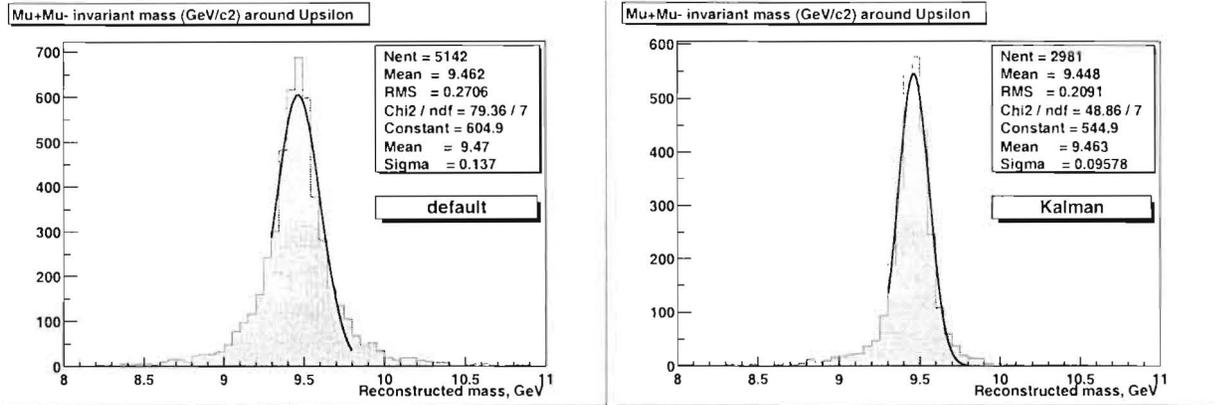
Figure 7: Reconstructed dimuon invariant mass for the case of "realistic" cluster finding and two background events: left) default tracking, right) Kalman filter.
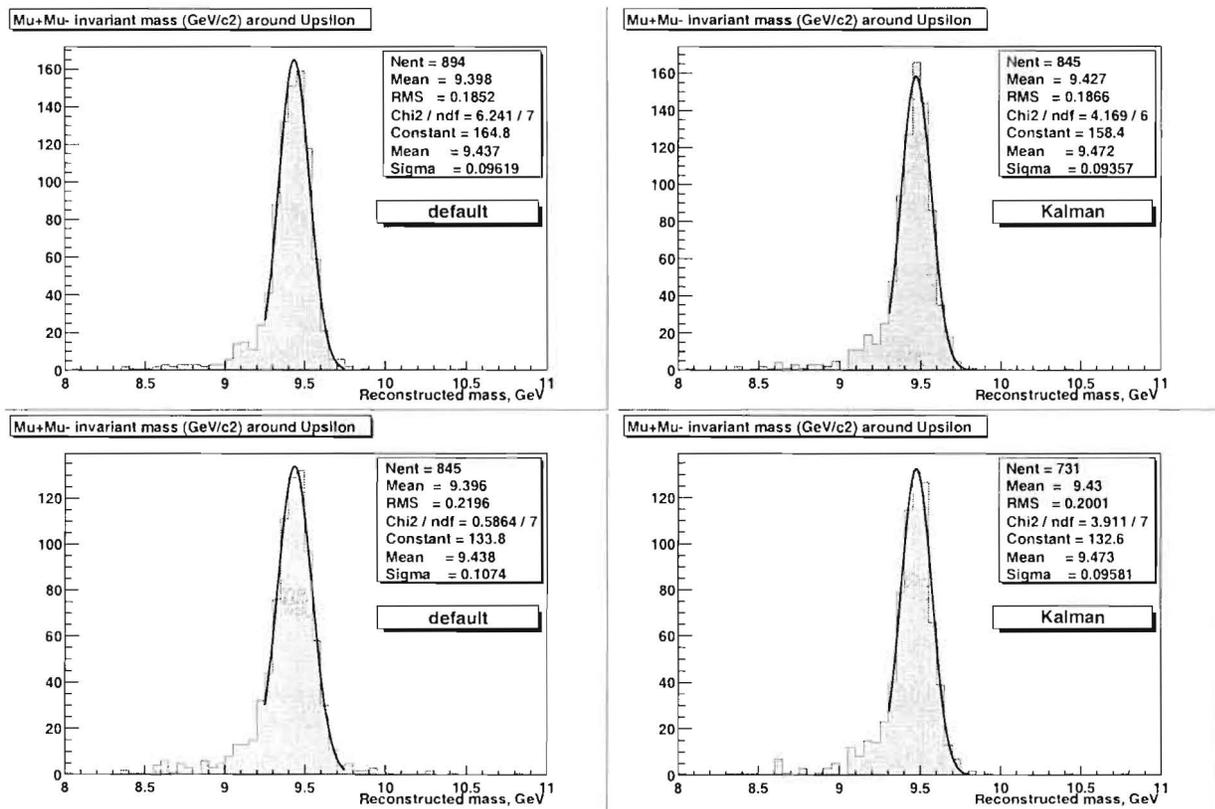
Figure 8: Reconstructed dimuon invariant mass for the case of new cluster finding: left) default tracking, right) Kalman filter, top) without background, bottom) with 2 nominal background events added.

13